SEISMIC PERFORMANCE OF STEEL SIDE PLATE MOMENT CONNECTIONS

C. C. Chou[1], K. C. Tsai[2], Y. Y. Wang[3], C. K. Jao[4]

[1] *Associate Professor, Dept. of Civil Engineering, Taiwan University, Taipei. Chinese Taiwan*
[2] *Professor, Dept. of Civil Engineering, Taiwan University, Taipei. Chinese Taiwan.*
Director of Center for Research on Earthquake Engineering(NCREE), Taipei, Chinese Taiwan.
[3] *President, P.E., SpringTech Engineering Consultant Inc., Taipei, Chinese Taiwan*
[4]*Former Graduate Student, Dept. of Civil Engineering, Chiao Tung University, Hsinchu, Chinese Taiwan*
Email: cechou@ntu.edu.tw, kctsai@ncree.org, spring.tech@msa.hinet.net

ABSTRACT :

Moment connections in a 34-story steel building located in Kaohsiung, Taiwan were rehabilitated to satisfy seismic requirements based on the 2005 AISC seismic provisions. Construction of the building was ceased in 1996 due to financial difficulties and was recommenced in 2007 with enhanced connection performance. Steel moment connections in the existing building were constructed by groove welding the beam flanges and bolting the beam web to the column. Four moment connections, two of which were removed from the existing 34-story steel building, were cyclically tested. A non-rehabilitated moment connection with bolted web-welded flanges was tested as a benchmark. Three moment connections rehabilitated by welding full-depth side plates between the column face and beam flange inner side were tested to validate the cyclic performance. Test results revealed that (1) the non-rehabilitated moment connection failed at an interstory drift of 3%, (2) all rehabilitated moment connections exhibited excellent performance, exceeding a 4% drift without fractures of beam flange groove-welded joints, and (3) two rehabilitated moment connections could be successfully tested twice with minor strength degradation. The connection specimens were also modeled using the non-linear finite element computer program ABAQUS to further confirm the effectiveness of the side plate in transferring beam moments to the column and to investigate potential sources of connection failure. A design procedure was proposed based on the experimental and analytical studies.

KEYWORDS: Rehabilitated Moment Connection, Side Plate, Cyclic Test, Finite Element Analysis

1. INTRODUCTION

Many traditional steel moment connections, which were fabricated following pre-Northridge construction practices with low notch toughness E70T-4 electrode, showed minimal plastic deformation before groove welded joint fractures. New moment connections, which either weaken or strengthen the beam section near the column face together with welding improvements, have been successfully tested, achieving large cyclic plastic deformation. Weakening schemes include the use of a reduced beam section or reduced flange plates near the beam-to-column interface to avoid groove weld fracture or beam buckling (Engelhardt et al. 1996, Chen et al. 1996, Chou and Wu 2007). Strengthening schemes include the use of cover plates, flange stiffeners, and haunches near the beam-to-column interface (Uang et al. 2000, Kim et al. 2002, Chou and Jao 2007).

The ER70S-G electrode, similar to the E71T-8 or E70TG-K2 electrodes, provides a minimum specified Charpy V-Notch value of 27 J at -29°C (20 ft-lbs at -20F), which is accepted by AISC (2005) for beam flange groove welds. Since the ER70S-G electrode is used to conduct the beam flange groove welds to the box column in Taiwan construction practices, the connection shows a better performance (e.g. 3% drift) than pre-Northridge moment connections utilizing the E70T-4 electrode. However, these connections still fail to satisfy connection cyclic performance, specified based on AISC (2005) and FEMA 350 (2000). This study provides a rehabilitation scheme for improving cyclic performance of steel moment connections, minimizing interference from the composite slab, and reducing story height requirements in the existing building (Jao 2007).

Cyclic testing was performed on four exterior moment connections, two of which were removed from

the existing 34-story steel building in Kaohsiung, Taiwan. A rehabilitation scheme was proposed to strengthen three connections by adding a pair of full-depth side plates between the column face and beam flange inner side. The side plates are intended to help transfer some beam moments to the column because existing beam flange groove welded joints could sustain modest inelastic deformation before fracturing (Tsai et al. 1995, Chou et al. 2006). No need is required to modify the existing groove welds of the beam top and bottom flanges, indicating no damages in an existing composite slab. This scheme differs from that utilizing the Side Plate connection (FEMA 350), which completely eliminates the reliance on existing beam flange groove welded joints at the column face for transferring beam moments. In this paper, test results that support the seismic performance of the rehabilitated steel moment connections are presented first; the key parameter is the side plate size. Next, the connection specimens are modeled using the non-linear finite element computer program ABAQUS (2003) to confirm the effectiveness of the side plate in transferring beam moments to the column.

2. REHABILITATED STEEL MOMENT CONNECTION

Fig. 1 shows a rehabilitated moment connection using a pair of side plates between the column face and beam flange inner side. These two side plates are used to transfer some beam flange force to the column to reduce beam flange strain and prevent groove weld fracture. The figure shows moment demand, M_{dem}, along the beam, assuming that a plastic hinge is located a quarter beam depth from the end of the side plates. The moment at the column face, as determined by projecting moment capacity M_{PH} at the plastic hinge location, is

$$M_{dem} = \frac{L_b}{L_b - (L_s + d_b/4)} M_{PH} = \frac{L_b}{L_b - (L_s + d_b/4)} \left(\beta R_y \sigma_{yn} Z_b\right) \tag{2.1}$$

where L_b is the distance from the mid-span to the column face; L_s is the side plate length; d_b is the beam depth; Z_b is the plastic section modulus of the beam; σ_{yn} is the specified yield strength of the steel; R_y is the material over-strength coefficient, and coefficient β ($\approx$1.3) denotes strain hardening (FEMA 350). Since steel properties were obtained from tensile coupon tests before fabricating rehabilitated specimens, actual yield strength (σ_y), actual tensile strength (σ_u), and R_y=1 were used in Eq. (2.1) to estimate moment demand, M_{dem}.

Moment capacity, M_{cap}, near the beam-to-column interface increases as a result of the side plates. Although the stress distributions near the beam-to-column interface are complicated, a simple bending theory is adopted to estimate the flexural capacity of the rehabilitated beam, which is the summation of the flexural strengths of the beam, M_{pb}, and the two side plates, M_{ps}:

$$M_{cap} = M_{pb} + M_{ps} = Z_b R_y \sigma_{yn} + \frac{1}{2}\left(d_b - 2t_f\right)^2 R_y \sigma_{yn} t_s \tag{2.2}$$

where t_f is the beam flange thickness and t_s is the side plate thickness. It is assumed that the side plates are subjected to top and bottom flange force, P_{sF}, as shown in Fig. 2(b), and exhibit a fully plastic stress state [Fig. 2(c)]. By considering moment equilibrium in the side plate, the force, P_{sF}, is:

$$P_{sF} = \frac{F_s\left[\frac{1}{2}\left(d_b - 2t_f\right)\right]}{d_b - 2t_f} = \frac{1}{4}\left(d_b - 2t_f\right) R_y \sigma_{yn} t_s \tag{2.3}$$

Additionally, the force P_{sF} is transferred to the side plate through shear on the groove welded joint between the side plate and beam flange inner side, and thus the minimum length of the side plate, L_s, is determined based on groove weld strength:

$$L_s \geq \frac{\frac{1}{4}\left(d_b - 2t_f\right) R_y \sigma_{yn}}{0.8(0.6F_{exx})} \tag{2.4}$$

where F_{exx} is the weld strength. Assuming the rehabilitated beam moment capacity-demand ratio,α ($=M_{cap}/M_{dem}$), is larger than one, the side plate thickness, t_s, can be calculated using Eq. (2.2):

$$t_s \geq \frac{\alpha M_{dem} - M_{pb}}{\frac{1}{2}\left(d_b - 2t_f\right)^2 R_y \sigma_{yn}} \tag{2.5}$$

3. TEST PROGRAM

3.1 CONNECTION SPECIMENS

The experimental program consisted of tests of four specimens, each of which represented an exterior moment connection with one steel beam and one welded box column. Table 1 lists the beam, column, and side plate sizes. ASTM Grade 50 steel was utilized for the column, continuity plate, and side plate; ASTM A36 steel was utilized for the beam. Specimens UR and SP1 were removed from the 33rd floor of the existing steel building located in Taiwan, while Specimens SP2 and SP3 were fabricated in the laboratory. Specimen UR, passing the ultrasonic weld test, represented an unreinforced bolted web-welded flange fully-restrained moment connection [Fig. 3(a)] and was tested as a benchmark. The beam flanges were groove-welded to the box column using the ER70S-G electrode, which is similar to the E71T-8 or E70TG-K2 electrodes. The steel backing was left in place for the top and bottom flange groove welds; no supplemental fillet welds were made between the steel backing and column. The shear plate was fillet welded to the column and bolted to the beam web; supplemental fillet welds were made between the beam web and the shear plate. Welding details were identical in all specimens, except that the supplemental fillet weld between the shear plate and the beam web was not adopted in all rehabilitated specimens. Specimen SP2 [Fig. 3(b)] was identical to Specimen SP3, except that (1) the side plate size was 22×300 mm in Specimen SP2 and 18×254 mm in Specimen SP3, and (2) Specimen SP3 had side plate length, L_s, less than the required value of 264 mm based on Eq. (2.4). The objective was to discover the possible failure mode in the rehabilitated connection. The rehabilitated beam moment capacity-demand ratio,α (=M_{cap}/M_{dem}), is 1.49 (SP1), 1.31 (SP2), and 1.27 (SP3) to study the effects of reinforcement on connection cyclic behavior and to discover the minimum reinforcement for the proposed connection.

Table 1. Member sizes and properties

Spe.	Column Size/ Beam Size (mm)	Column Strength		Beam Flange Strength		Beam Web Strength		Side Plate (mm) (t_s×L_s)	Side Plate Strength	
		σ_y (MPa)	σ_u (MPa)	σ_y (MPa)	σ_u (MPa)	σ_y (MPa)	σ_u (MPa)		σ_y (MPa)	σ_u (MPa)
UR	□700×700×35×35 H702×254×16×28	391	525	275	485	288	495	-	-	-
SP1	□700×700×35×35 H688×255×13×21	391	525	250	418	385	437	20×300	400	557
SP2	□550×550×35×35 H702×254×16×28	385	530	250	418	280	437	22×300	370	500
SP3	□550×550×35×35 H702×254×16×28	385	530	251	413	281	434	18×254	400	532

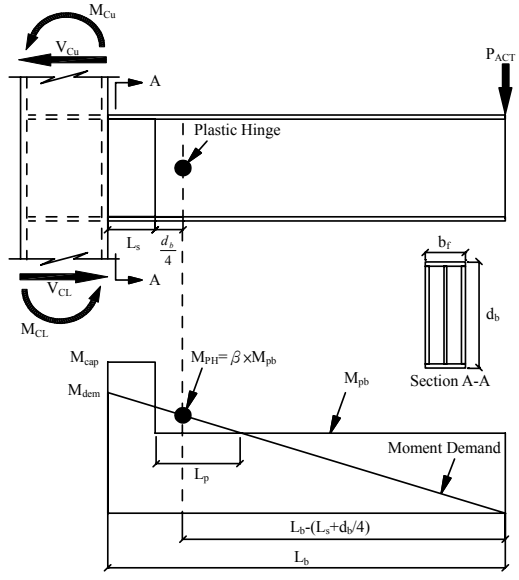

Figure 1 Moment capacity and demand along a beam axis

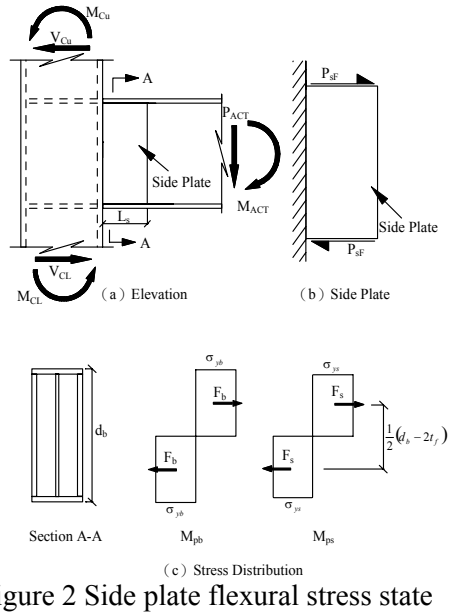

Figure 2 Side plate flexural stress state

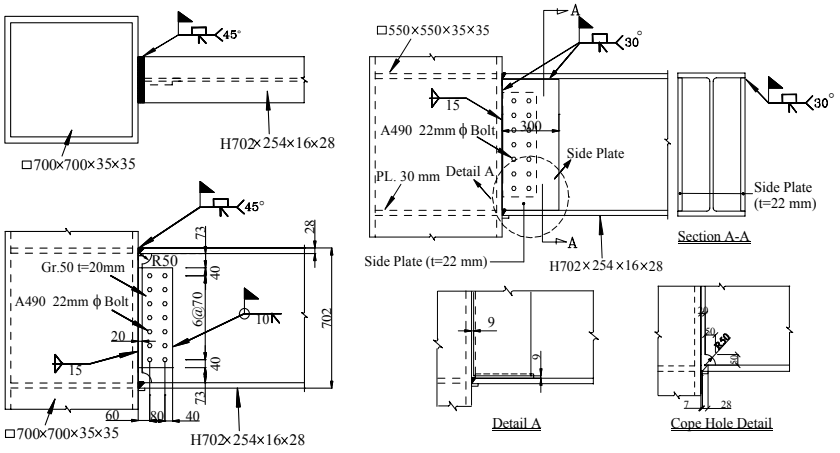

（a）Specimen UR （b）Specimen SP2

Figure 3 Connection details

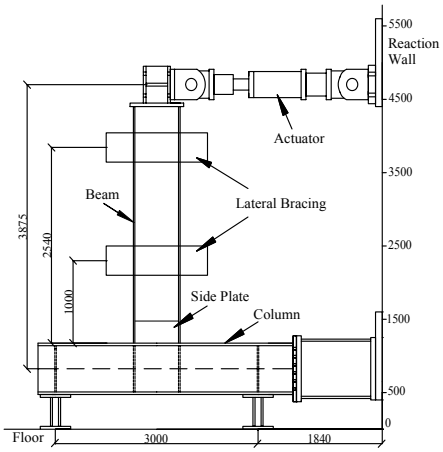

Figure 4 Test setup

3.2 TEST SETUP AND LOADING PROTOCOL

The exterior connection specimens were tested as shown in Fig. 4. Restraint to lateral-torsional buckling of the beam was provided near the actuator and at a distance of 1000 mm from the column face. Displacements were imposed on the beam by a 1000 kN actuator at a distance of 3875 mm from the column centerline. The AISC cyclic displacement history was used and run under displacement control. Specimens were tested until connection failure occurred or limitations of the test setup were reached.

4. TEST RESULTS

4.1 NON-REHABILITATED MOMENT CONNECTION

Fig. 5(a) shows the global response of Specimen UR; the moment computed at the column face is normalized by the nominal plastic moment of the beam, M_{np}. Whitewash flaking was observed in the beam flange at an interstory drift of 0.75%, indicating beam yield. A minor fracture of the groove weld in the beam top flange and fillet weld between the shear plate and column face occurred at an interstory drift of 3%. However, the peak strength was maintained at this drift level. Strength decreased significantly towards an interstory drift of -4% due to beam top flange fracture. No column or panel zone yielding was observed throughout the test.

4.2 REHABILITATED MOMENT CONNECTION

Fig. 5(b) shows the hysteretic responses of Specimen SP1, which achieved high interstory drift without welded joint fracture. Beam outside the end of the side plate yielded at an interstory drift of 0.75-1%. Minor beam buckling occurred at an interstory drift of 2%, and significant beam buckling occurred at a maximum interstory drift of 4.7%. No groove weld fracture at the beam-to-column interface occurred.

Figs. 5 (c)-(d) show the hysteretic responses of Specimens SP2-3, respectively. Since beam strength degradation was not observed after the first cyclic test beyond an interstory drift of 4%, both specimens were retested using the same AISC loading protocol (2005). Fig. 6(a) shows the beam deformation of Specimen SP2 after the first test to an interstory drift of 4.4%; flange and web buckling amplitudes were about 14 mm and 16 mm, respectively, much smaller than those observed in the Specimen SP1 test. Minor yielding was observed at the side plate near the beam-to-column interface; minor cracks were also observed at the beam flange ends near the groove welded joint but did not affect the connection performance. When Specimen SP2 was retested to an interstory drift of 1%, minor flange cracks near the end of the side plates were observed due to flange local buckling. At the end of 4% drift cycles, the crack length increased to 10 mm and significant beam buckling was noted [Fig. 6(b)], leading to slight strength degradation [Fig. 5(c)]. No weld fracture between the beam-to-column interface was observed after the second cyclic test. Specimen SP3 was identical to Specimen SP2 except that Specimen SP3 had a small side plate and an insufficient side plate length (Table 1). No beam buckling was observed after the specimen finished 4% drift cycles. However, a minor crack was observed at the end of the groove weld between the beam flange inner side and the side plate. Beam buckling was difficult to

detect even when testing to an interstory drift of 4.8%. When Specimen SP3 was retested to an interstory drift of 1%, a minor crack was observed near the beam-to-column groove welded joint. This crack remained minor even after finishing 3.77% drift cycles. However, the crack at the end of the groove weld between the beam flange inner side and the side plate propagated along the weld due to beam flange local buckling. The crack length was 70 mm at the end of the second test [Fig. 6(c)], and slight strength degradation was also noted in the hysteretic loops [Fig. 5(d)].

Table 2 lists moment demands, M_{dem} and M_{PH}, calculated by multiplying the actuator force and the distance to the column face and plastic hinge location, respectively. The flexural strengths, M_{cap} and M_{pb}, were calculated using true material strength according to Eq. (2.2). The rehabilitated beam moment capacity-demand ratio,α ($=M_{cap}/M_{dem}$), ranges from 1.11 to 1.56 while the strain-hardening coefficient β ranges from 1.28 to 1.54. Note that Specimen SP1 has smallest β value among all of the specimens because of significant beam buckling for limiting strain hardening. However, minor beam buckling was observed in Specimens SP2 and SP3 in the first test, leading to β values of approximately 1.5, higher than that calculated based on FEMA 350 (2000). Note that for high column flexural stiffness and high reinforcement near the beam-to-column interface (α>1.5 for Specimen SP1 in Table 2), the beam buckling amplitude is large and the rate of degradation of moment resistance is high in the test. Conversely, when a column is relatively soft with relatively low reinforcement near the beam-to-column interface (α=1.11-1.16 for Specimens SP2 and SP3 in Table 2), the beam buckling amplitude is much smaller and the rate of degradation of moment resistance is also slower in the test.

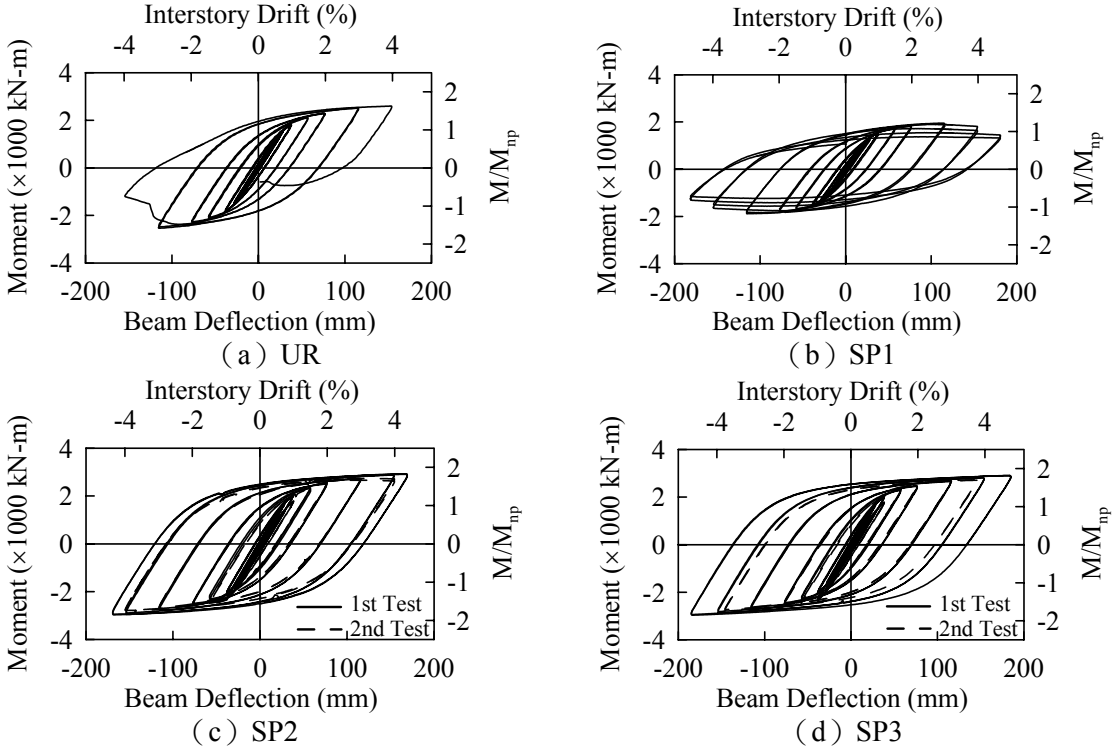

Figure 5 Beam moment-deflection responses

(a) SP2 first test (4.4% drift) (b) SP2 second test (4% drift) (c) SP3 After second test

Figure 6 Specimens SP2 and SP3 observed performance

Table 2. Parameters α and β based on test results

Specimen	Interstory Drift (%)	Moment Demand (kN-m)		Flexural Strength (kN-m)		Parameters α and β	
		Column Face M_{dem}	Plastic Hinge M_{PH}	Column Face M_{cap}	Plastic Hinge M_{pb}	$\alpha = \frac{M_{cap}}{M_{dem}}$	$\beta = \frac{M_{PH}}{M_{pb}}$
UR	+3	2516	2516	1799	1799	0.72	1.4
	-3	-2517	-2517			0.72	1.4
SP1	+4	1885	1633	2942	1273	1.56	1.28
	-4	-1952	-1691			1.51	1.33
SP2	+4	2948	2559	3364	1666	1.14	1.54
	-4	-2896	-2514			1.16	1.51
SP3	+4	2866	2524	3175	1672	1.11	1.51
	-4	-2830	-2492			1.12	1.49

5. FINITE ELEMENT STUDY

Finite element analysis was undertaken to study the cyclic behavior of rehabilitated moment connections. The objective was to verify test results, discover flexural contribution of the side plates, and study sources of potential failure mode. The yield and tensile strengths of the weld metal obtained from the fabricator were 469 and 563 MPa, respectively. The analyses accounted for material nonlinearities, using the von Mises yield criterion. Fig. 7(a) shows von Mises stress contours of Specimen SP2 at an interstory drift of 3%, indicating stress concentration near the top and bottom sides of the side plate. Fig. 7(b) compares beam moment-deflection hysteretic responses from testing and analysis. The predicted longitudinal strains along the side plate depth, located 35 mm from the column face, correlate well with the test data (Fig. 7(c)). The longitudinal strains in the side plate center portion are small, indicating ineffective in transferring beam flange forces to the column. The longitudinal strains in the side plate near the beam flanges are greater than the yield strain, indicating effective in transferring beam flange forces. Therefore, utilizing four flange stiffeners between the beam flange inner side and the column face is also a successful rehabilitation scheme for the steel moment connections (Chou and Jao 2007). From the finite element model, moment, M_s, transferred through the side plate to the column, was computed based on the longitudinal stresses in the side plate, the respective area along the depth, and the distance to the beam web centerline. The ratio of M_s to beam moment, M_{ABA}, computed at the column face, was 36-38% at an interstory drift of 4% (Fig. 8), indicating that about one third of the beam moment was transferred to the column through the side plates, and Specimen SP2 utilizing thicker side plates than Specimen SP3 transferred larger beam moments. The rupture index (RI) was computed at different locations of the connection from ABAQUS results to assess the possible fracture source. Locations in a connection with higher values for RI have a greater potential for fracture. A study was conducted to investigate the effects of side plate size on RI distributions at the likely fracture location (the groove-weld top surface near the column face). Nine different side plates were used to reinforce the connection in Specimen SP2, and the material properties of the side plate in Specimen SP2 were also used. The rehabilitated beam moment capacity-demand ratio, α, in these models ranged from 0.94-1.20. Fig. 9 shows that the RI variation is inversely dependent on side plate thickness, t_s, and weakly dependent on side plate length, L_s, indicating that the increase in the side plate thickness can effectively reduce the RI value.

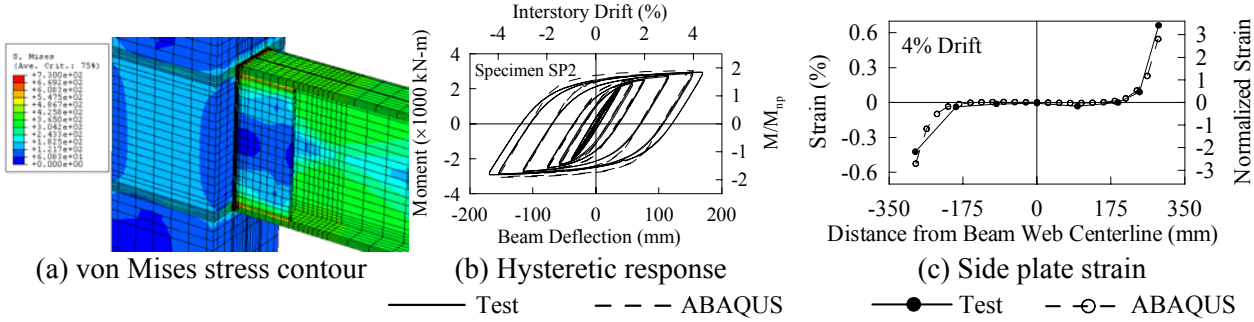

(a) von Mises stress contour (b) Hysteretic response (c) Side plate strain

Figure 7 Finite element analysis for Specimen SP2

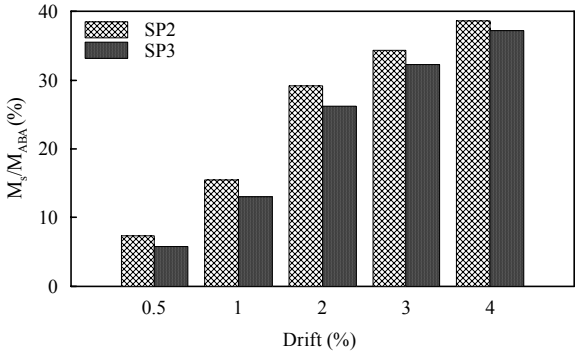

Figure 8 Side plate moment contribution

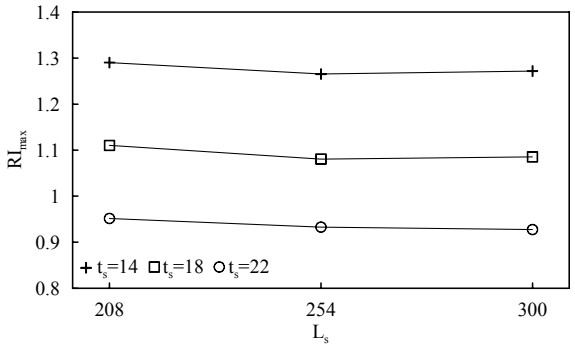

Figure 9 Maximum RI value on groove welded joint

6. SUMMARY OF SIDE PLATE MOMENT CONNECTION DESIGN PROCEDURE

A design procedure for the seismic rehabilitation of a bolted web-welded flange moment connection was developed based on experimental and analytical studies in this research. The details of a non-rehabilitated fully-restrained moment connection are: (1) beam flange groove welds are made using a high notch toughness electrode (e.g. ER70S-G, E71T-8, or E70TG-K2 electrodes) with steel backing left in place, (2) the beam web is bolted to the column shear plate, and (3) continuity plates in the box column are at least as thick as the beam flange. Due to limited test data available for this type connection, the box column width should be less than 2.8 times the beam width, and the column thickness should be larger than 1.25 times the beam flange thickness to maintain locally stiff column relative to the beam. The step-by-step design procedure is summarized as follows:

Step 1: Select a side plate length, L_s, based on the beam dimension and strength [Eq. (2.4)].
Step 2: Compute the beam plastic moment at the column face using a strain hardening factor, β, of 1.5 [Eq. (2.1)].
Step 3:Use Eq. (2.5) to compute the side plate thickness with a rehabilitated beam moment capacity-demand ratio, α, larger than 1.11.

7. CONCLUSIONS

Four exterior moment connection specimens, each composed of an ASTM A572 Gr. 50 welded box column and an ASTM A36 wide-flange beam, were cyclically tested. Two bolted web-welded flange moment connections, prequalified for Ordinary Moment Frames (AISC 2005), were removed from an existing 34-story steel building in Taiwan. One of the connections was rehabilitated by welding two side plates between the column face and the inside of the beam flange to improve seismic performance. Additional two rehabilitated moment connection specimens were fabricated in the laboratory. Note that the ER70S-G electrode, which is similar to the E71T-8 or E70TG-K2 electrodes, was used to make beam flange groove welds in all connections based on construction practices in Taiwan. Steel backing was left in place for the top and bottom flanges and no supplemental fillet welds were made between the steel backing and the column face. The following can be concluded based on the experimental and finite element analysis results.

1. Fracture of the beam flange near the column face was the failure mode for the non-rehabilitated Specimen UR. The interstory drift angle was 3% and the maximum tensile strain was about 3-4%.
2. Maximum moment developed at a quarter beam depth from the end of the side plate was 1.28-1.54 times the actual beam plastic moment. The strain hardening of around 1.5 exceeded that calculated based on FEMA 350 (2000) due to minor beam buckling at the plastic hinge location. In the absence of additional connection tests, a strain hardening factor of 1.5 for A36 beams was recommended for estimating the rehabilitated connection moment at the plastic hinge location.
3. The flexural capacity of the rehabilitated beam was the sum of the plastic moments of a non-rehabilitated beam and two side plates. The rehabilitated beam moment capacity-demand ratio, α, at the column face ranged from 1.11-1.56 for three rehabilitated connection specimens at an interstory drift of 4%. For Specimen SP1, which had an α value larger than 1.5, significant beam buckling was observed in the first

cyclic test at an intersotry drift of 4.8%, but no weld fracture was observed at the beam-to-column interface. For Specimens SP2 and SP3, which had α values ranging from 1.11-1.16, minor beam buckling was observed in the first cyclic test after an interstory drift exceeded 4%. These specimens were retested using the same AISC cyclic loading protocol, and no fracture of the beam flange groove-welded joint at the column face was observed after the second cyclic test. However, because Specimen SP3 had insufficient side plate length, the weld fractured along the junction between the side plate and the beam flange inner side. It is recommended that α value larger than 1.11 be used to determine side plate size.

4. Finite element analysis showed that the side plates could transfer approximately one third of the beam moments to the column, and increasing the side plate thickness could significantly reduce beam flange RI demand at the beam-to-column interface.

ACKNOWLEDGEMENTS

The test program was supported by the Chiao Tung University, Center for Research on Earthquake Engineering (NCREE), and Spring Consulting Company, Chinese Taiwan.

REFERENCES

American Institute of Steel Construction AISC. (2005). *Seismic provisions for structural steel buildings*, Chicago, IL.

Chou, C-C, Wu, C-C, Jao, C-K, and Wang, Y-Y. (2006). Weakened and strengthened steel moment connections. *4th International Conference on Earthquake Engineering*, Paper No: 152, Taipei, Chinese Taiwan.

Chou, C-C and Wu, C-C (2007). Performance evaluation of steel reduced flange plate moment connections. *Earthq. Engrg. Struct. Dyn.,* 36, 2083-2097.

Chou, C-C and Jao, C-K (2007). Seismic rehabilitation of steel moment connections utilizing flange internal stiffeners. *2nd International Conference on Urban Disaster Reduction*, Taipei, Chinese Taiwan.

Chen, S-J, Yeh, C-H, and Chu, J-M (1996). Ductile steel beam-to-column connections for seismic resistance. *J. Struct. Engrg.*, ASCE. 122(11): 1292-1299.

Engelhardt, M.D., Winneberger, T., Zekany, A.J., and Potyraj, T. (1996). The dogbone connection: Part II. *Modern Steel Construction*. AISC.

Federal Emergency Management Agency FEMA. (2000). *Recommended seismic design criteria for new steel moment-frame buildings*, *Rep. No. FEMA 350*. Washington, D.C.

HKS. (2003). *ABAQUS User's Manual Version 6.3*, Hibbitt, Karlsson & Sorensen, Pawtucket, RI.

Jao, C-K (2007). Seismic behavior of steel retrofitted moment connections with stiffeners inside beam flange, *Thesis advisor: Chou C-C*, Chiao Tung University, Hsinchu, Chinese Taiwan.

Kim, T., Whittaker, A.S., Gilani, A.S.J., Bertero, V.V., and Takhirov, S.M. (2002). Experimental evaluation of plate-reinforced steel moment-resisting connections, *J. Struct. Engrg.*, ASCE, 128(4), 483-491.

Tsai, K-C, Wu S., and Popov E.P. (1995). Experimental performance of seismic steel beam-column moment joints, *J. Struct. Engrg.*, ASCE, 126(6), 925-931.

Uang, C-M, Yu, Q-S, Noel, S., and Gross, J. (2000). Cyclic testing of steel moment connections rehabilitated with RBS or welded haunch, *J. Struct. Engrg.*, ASCE, 126(1), 57-68.